Active Operation of Hydrogen Fuelling Stations to Support Renewable Integration

Citation for published version:
Sun, W & Harrison, G 2018, Active Operation of Hydrogen Fuelling Stations to Support Renewable Integration. in *2017 IEEE PES Innovative Smart Grid Technologies Conference Europe (ISGT-Europe).* IEEE, PES Innovative Smart Grid Technologies Conference Europe (ISGT-Europe) 2017, Turin, Italy, 26/09/17. https://doi.org/10.1109/ISGTEurope.2017.8260194

Digital Object Identifier (DOI):
10.1109/ISGTEurope.2017.8260194

Link:
Link to publication record in Edinburgh Research Explorer

Document Version:
Peer reviewed version

Published In:
2017 IEEE PES Innovative Smart Grid Technologies Conference Europe (ISGT-Europe)

Active Operation of Hydrogen Fuelling Stations to Support Renewable Integration

Wei Sun
University of Edinburgh
Edinburgh, UK
w.sun@ed.ac.uk

Gareth Harrison
University of Edinburgh
Edinburgh, UK
gareth.harrison@ed.ac.uk

***Abstract*——To reduce carbon emissions in the transportation sector, the deployment of hydrogen Fuel Cell Electric Vehicles (FCEV) is an alternative to battery Electric Vehicles. Green hydrogen fuel can be generated by converting low carbon electricity at refuelling stations equipped with water electrolysis, especially in renewable rich areas. The fast response capability of electrolysis, coupled with onsite hydrogen tanks, could potentially turn the station demand into a flexible load since the hydrogen can be stored and used when needed. This paper describes a scheme for actively operating hydrogen fuelling stations in renewable rich areas, providing flexible response to manage constraints and release network headroom for connecting renewable generation. Under this operational approach, electrolysers at the hydrogen fuelling station adaptively increase electricity consumption (i.e. overproduction) to overcome thermal overloading issues near the point of connection, and then subsequently reduce electricity consumption (i.e. under-production) to release the unscheduled hydrogen stored in onsite tanks. The results of a case study in a 11 kV distribution network are presented. Based on the results, the effectiveness of actively station operation is demonstrated with considerable reductions in curtailment.**

***Index Terms*—active network management, thermal management, hydrogen production and storage, hydrogen vehicle, multi-energy integration**

I. INTRODUCTION

The deployment of hydrogen (H_2) fuelled vehicles (FCEV) is a potentially attractive and effective approach to reduce carbon emissions and dependency on fossil fuels. The roll-out of hydrogen-fuelled vehicles in the UK has already begun, although in relatively limited numbers. Recent years have seen deployment of large demonstration fleets of hydrogen-fuelled buses, as well as fuel cell passenger cars. These fleet deployments are accompanied by development of fuelling stations. The UK has two of the largest stations in Europe, with plans to expand the number of stations in the coming years [1].

While some advocate hydrogen networks based around large scale generation and transport of hydrogen, fuel at the hydrogen fuelling station could be generated by on-site electrolysis that consumes electricity from the local electricity network; there are several trials in the UK looking at this [2, 3].

In distribution networks that already operate near thermal capacity, the electricity consumption of refuelling station would be challenging to accommodate, due to rise in peak demand. Exploring the flexibility of on-site electrolysis to shave peak demand would be a potential solution in these cases. Distribution networks in renewable rich areas, such as Scotland, are struggling to accommodate more wind or PV installations without (major) network reinforcement. The constraints in these networks are due to electricity export from local generation rather than import. When deploying hydrogen fuelling station in these areas, controlling electrolysis power demand could be used as a means to provide potential headroom to connect new renewable generation. In addition, the use of on-site hydrogen storage tanks, which are competitive against battery storage of electricity for longer time scales and greater storage quantities [4], the fuelling station electricity consumption can be decoupled from its fuel demand for a considerable duration. The potential value of shaving peak demand and also supporting renewable integration from hydrogen fuelling stations would be further enhanced.

Operation and control of hydrogen fuelling stations has been studied from a number of different aspects, typically categorised by whether analysis considers connection to the main electricity network or operation as part of an islanded microgrid. Without explicitly considering where the electricity came from [5] looked at minimising the overall energy consumption while [6] minimised refuelling time. In the context of renewable integration, the studies on hydrogen fuelling stations can further split into: study at aggregated national level [7, 8]; or detailed study of individual stations accommodated in local distribution networks. For example, Carr et al. investigated the power management of electrolysers at fuelling stations using optimal power flow considering renewable generation [9] and with an extension to include market prices [10]. However, implementing OPF-based control approaches would require communications, measurement infrastructure and a centralized controller

The work has been funded by EPSRC, UK, through the ‘Hydrogen’s Value in the Energy System (HYVE)’ project (EP/L018284/1).

Active control for network constraint management, in general, is a very active research area. A series of centralised and decentralized approaches have also been proposed. These advanced control schemes aim to manage constraints to maximize use of the existing assets, release extra headroom for new demand and more renewable DG, although few consider hydrogen fuelling stations. Zhou and Bialek [11] present a generation curtailment approach for multiple DG units to manage voltage constraints. A decentralized control strategy is proposed in [12] to mitigate voltage rise and line overloads to facilitate increased connections of wind generation. It uses both reactive power control and generation curtailment in a real-time sensitivity method that tackles constraints local to the DG connection. Robertson et al. [13] developed more sophisticated OPF-based real-time scheduling for network control settings to better integrate high levels of DG, in a coordinated and synchronised manner. A centralized control algorithm is developed and trialled in [14], which uses limited information to manage EV charging points to mitigate simultaneous thermal and voltage problems in LV networks.

The work presented here proposes the concept of an active operational strategy capable of real-time management of electrolyser inputs to solve thermal constraints near the point of connection, without high levels of communication or a central controller for coordination. The control framework used in this paper is an extension of the work in [12], using a similar real-time sensitivity method to calculate the operating point, but mainly focuses on explicitly considering the flexible operation of hydrogen fuelling stations in renewable rich areas.

The paper is structured as follows: basic hydrogen fuelling station operation is introduced first and then the conceptual design of active control strategies are described. The validation of the proposed strategy through a case study are also presented and discussed.

II. Operating Strategies for H_2 Fuelling Stations

The distribution network with connections to hydrogen fuelling stations can be schematically presented as in Fig. 1. Electrolysers consume electricity from the local electricity network to produced hydrogen, in order to meet the fuelling demand of FCEV cars. The hydrogen produced is compressed first, and then either used to directly fill FCEV car tanks or is stored onsite and dispensed when needed. The process of converting electricity to compressed hydrogen is subject to energy losses and also needs to consider other engineering constraints such as the requirement for purity, etc.

The main operating purpose of the fuelling station is to meet the demand from the FCEV served. This aim can be achieved through a relatively simple and straightforward operational strategy (termed here as 'passive mode'). Beyond this fundamental operational target, and with the support of onsite storage, the refuelling station could also be operated in alternative modes, in order to serve other technical and economic targets in addition. This might include stabilising electrolyser production to ease wear and tear on the equipment, and adaptively adjusting electrolysers' scheduled power input to provide electricity network support. Three different strategies are discussed that become progressively more complex.

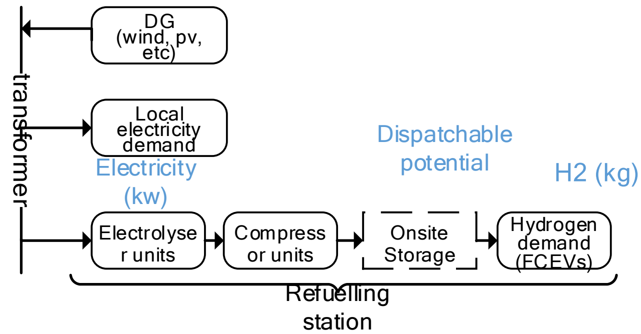

Figure 1. Generic model of the hydrogen refuelling station with power-to-gas production and grid connection

A. Passive operation mode

The passive model is presented first since it does not require storage. Here the (electrical) power input to electrolysers at the fuelling station ($P_{h2,t}$) aims to produce only the necessary amount of hydrogen demanded by FCEVs in each period *t* as:

$$P_{h2,t} = \frac{H2_{dem,t}}{HHV_{h2} \cdot \eta_{h2} \cdot \tau_t} \tag{1}$$

Here η_{h2} is the overall efficiency of hydrogen production, taking into account the energy loss of electrolyser units and also the compression and purification procedure. $H2_{dem,t}$ is the hydrogen fuel demand (kg) of the served FCEVs. HHV_{h2} is the higher heating value of hydrogen fuel (39.41 kWh/kg) and is used to convert fuel demand mass (in kg) into units of energy (in kWh); τ_t is the duration of period *t*.

Clearly, under this passive mode, hydrogen generation and demand would match in each period and therefore no storage is needed. The varying characteristics of hydrogen production here would require a large electrolyser to be installed to meet the peak hydrogen demand that may only occur few times over the year. Nevertheless, the continuously changing profile of electrolyser production would also cause wear and tear of the equipment and reduce its lifetime.

In practice, storage may be installed to buffer any mismatch within period *t*, but it is relatively small and therefore not considered here. In this paper only multiple hour storage capacity is considered which is used to balance the mismatch between each period.

B. Steady operation mode (with storage support)

Rather than varying its output, operating the fuelling station at a fixed electricity consumption rate has advantages in reducing the required size of the electrolyser, as well as its wear and tear. A 'steady operation' strategy is proposed to maintain production at a fixed value throughout the day, with the amount calculated based on the hourly average of the total hydrogen demand in the day:

$$P_{h2,t} = \frac{1}{24} \sum_{t=1}^{T} \frac{H2_{dem,t}}{HHV_{h2} \cdot \eta_{h2}}. \tag{2}$$

Owing to the variation in the number of FCEVs served at each period *t*, the mismatch between the electrolyser production and actual hydrogen demand will need be offset by onsite hydrogen storage. The changed status of hydrogen storage $SOC_{h2,t}$ at the end of each period, can be calculated as:

$$SOC_{h2,t} = SOC_{h2,t-1} + P_{h2,t} \cdot \eta_{h2} \cdot \tau_t - \frac{H2_{dem,t}}{HHV_{h2}} \cdot \quad (3)$$

If the demand is correctly foreseen, at the end of the day, the storage will return to the initial start-of-day level.

C. Active operation mode with network constraint management

The electrolyser has the capability to rapidly change its operation point within a few seconds [4]. With adequate onsite hydrogen storage tanks, the fuelling station can quickly respond to the network issues. An active response approach, on top of normal operation, is proposed here aiming to provide constraint management for the local electricity network. This control approach is schematically illustrated in Figure 2, and will be explained in detail in the following sections.

It is important to point out that the overloading event considered here is caused by exporting power to the upper level network due to high DGs penetrations. Therefore, increasing refuelling station demand will tend to relieve congestion by consuming more DG output locally, which is opposite to the case where overloading is caused by local peak demand.

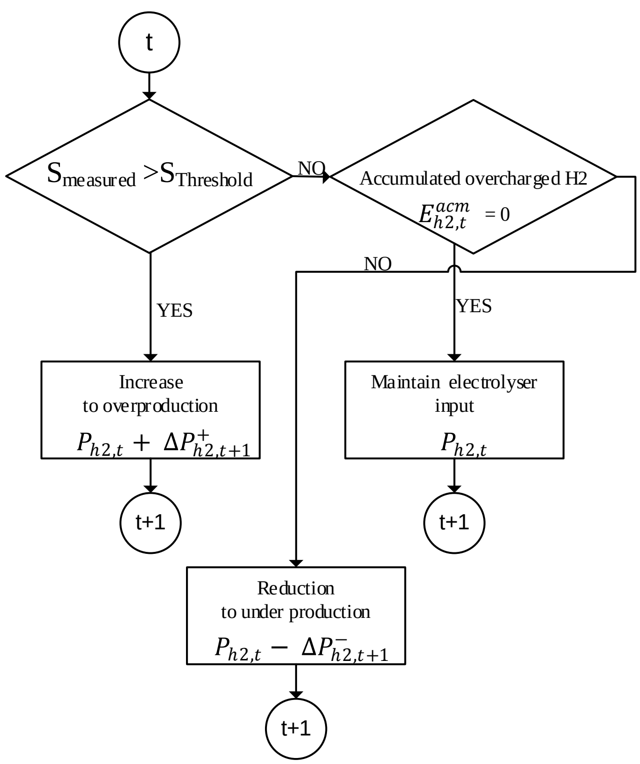

Figure 2. Schematic of control flow of active operational approach

1) Normal operation

The normal operational state of the fuelling station is based on the predefined operating points, and would be expected to dominate the operation period. Unless there is a network constraint, the electrolysers will continue to operate at the (day ahead) scheduled value, defined by (2).

2) Overproduction

When the overloading event is observed at the monitoring feeder/transformer nearby at time step *t*, the overproduction decision-making process for the next time step *t*+1 is activated to consume more electricity locally by increasing hydrogen production. The electrolyser's power input is set to an overcharging value $P_{h2,t+1}$ in the following time step, calculated as (4). The increased station power consumption $\Delta P^{+}_{h2,t}$ in (5) is estimated using the sensitivity of the line flow at the congestion feeder/transformer to the refuelling station's power input ($\delta S_t \,/\, \delta P_{h2,t}$) [12].

$$P_{h2,t+1} = P_{h2,t} + \Delta P^{+}_{h2,t+1} \quad (4)$$

$$\Delta P^{+}_{h2,t+1} = \frac{S_{measured,t} - S_{targeted}}{\delta S_t \,/\, \delta P_{h2,t}} \quad (5)$$

While the increased electrolyser power demand $P_{h2,t+1}$ attempts to relieve the observed overloading at the congested feeder/transformer, its final value will be subject to two other factors: the rated power of the electrolyser (P^{+}_{h2}) as (6) and the remaining free onsite storage capacity as (7), where E^{rated}_{st} is the total capacity of the hydrogen tank (MWh). The minimum of the three factors in (4,5,6) determines the final increased input for overcharging.

$$P_{h2,t+1} \leq P^{+}_{h2} \quad (6)$$

$$P_{h2,t+1} \leq \frac{E^{rated}_{st} - SOC_{h2,t}}{\tau_t} \quad (7)$$

It is also important to record the accumulated 'overproduced' hydrogen ($E^{acm}_{h2,t}$) in the storage tanks at the end of overproduction as (8), so as to indicate the following actions to restore the SOC level back due to its intended value.

$$E^{acm}_{h2,t+1} = E^{acm}_{h2,t} - \Delta P^{+}_{h2,t} \cdot \eta_{h2} \cdot \tau_t \quad (8)$$

3) Underproduction

After the overproduction period, the unscheduled extra hydrogen is stored in the onsite storage. This amount of overcharged hydrogen would need to be released soon so that the onsite storage can return to its planned position and provide support for the upcoming periods. To do so, electrolysers will undertake a period of underproduction to reduce the amount of overstored hydrogen

The decision-making process for electrolyser underproduction is triggered at the end of time step *t* if the previously accumulated overproduced hydrogen storage has not been fully released (i.e. $E^{acm}_{h2,t} \neq 0$). For the next time step *t*+1, the reduction ($\Delta P^{acm}_{h2,t+1}$) aims to release overproduced hydrogen; the electrolyser input is calculated as:

$$\Delta P_{h2,t+1}^{acm} = \frac{E_{h2,t}^{acm}}{\tau_t} \quad (9)$$

$$P_{h2,t+1} = P_{h2,t} - \Delta P_{h2,t+1}^{acm} \quad (10)$$

Opposite to the overproduction action, the underproduction from the electrolyser will increase the loading of the primary transformer nearby, as a result of less local electricity consumption and more DG output being exported. This potential adverse impact must be taken into account, and thus is limited by network capacity at this period calculated by (11) The maximum allowed reduction $\Delta P_{h2,t+1}^{-}$ is estimated using the sensitivity method in (12). Nevertheless, electrolyser input may not be allowed to reduce to zero to avoid complete turn down. The minimum allowed electrolyser operation level $P_{h2}^{-}$is also considered as a limit, included as the last item in (13).

$$P_{h2,t+1} \geq P_{h2,t} - \Delta P_{h2,t+1}^{-} \quad (11)$$

$$\Delta P_{h2,t+1}^{-} = \frac{S_{targeted} - S_{measured,t}}{\delta S_t \mathbin{/} \delta P_{h2,t}} \quad (12)$$

$$P_{h2,t+1} \geq P_{h2}^{-} \quad (13)$$

The new electricity input $P_{h2,t+1}$will finally be calculated based on the maximum of the three factors in (10,11,13). At the end of the undercharging period, $E_{h2,t+1}^{acm}$ is also updated accordingly.

III. CASE STUDY

To examine the fuelling station control strategies, a simplified 5 bus network presenting a distribution network in a wind rich area is studied. The demand and transformer data is based on typical 11 kV network. Peak demand (excluding fuelling station demand) is 3MW and there is a 6MVA transformer connecting to the higher voltage network.

The fuelling station's peak day hydrogen fuel demand is assumed to be 560kg, based on 100 FCEVs being refilled, using 5.6 kg on average to fill their tanks. The total efficiency due to the losses from producing hydrogen through to filling the FCEV tanks is set as 63% [10].

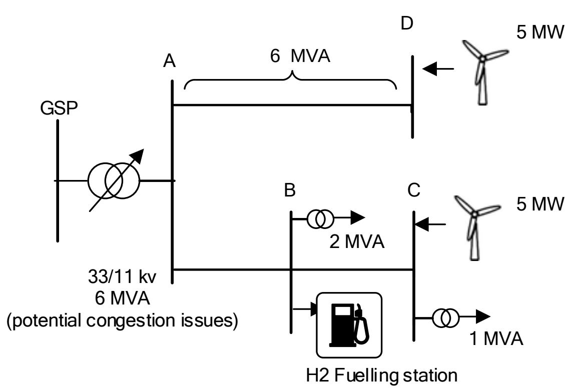

Figure 3. 11kV network case in wind rich area with hydrogen fuelling station connected

A week long half hourly time series for the hydrogen demand level at a fuelling station is shown in Figure 4. This is shown as the percentage of peak day total, and derived from a modified Chevron™ profile in the H2A analysis [15]. The original profile is adjusted to represent station closure during the night.

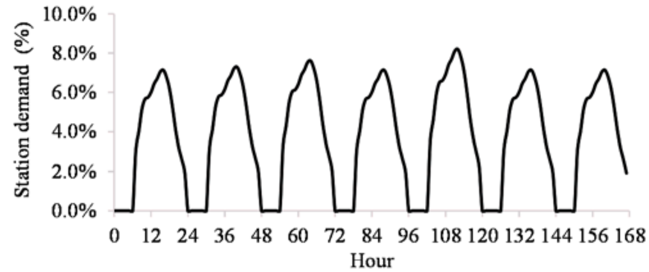

Figure 4. Half-hourly fuelling station hydrogen demand over a week (Monday to Sunday)

Applying the time series mentioned above, the half hourly equivalent electricity demand of the fuelling station can be calculated, which peaks at 2.9 MW at Friday noon. Electrolysers at the station correspondingly have a rated power of 2.9 MW. The onsite storage is assumed to have a day's capacity (35 MWh).

There are two wind farm in the network. A firm wind farm of 5 MW is connect at bus D, exporting as much as it generates. Another more flexibly connected wind farm at bus C is rated at 5 MW with unity power factor, which is well beyond the 2 MW capacity that fit-and-forget operation of the network can host. It is necessary to curtail this wind farm to avoid network constraints, namely the overloading issues at the primary transformer during strong wind periods. Demand and wind speed data for central Scotland in 2003 is used.

A. *Validation of operation strategies in 1 hour window*

The simulation of a 1 hour window at 1 minute steps is studied first in detail. The primary transformer is assumed to have a control threshold of loading of 95% above which active control is required. As shown in Figure 5, within this hour, the overloading of the primary transformer starts to constantly occur from 08:50. At 08:50, the electrolyser is operating at 1.03 MW (its predefined average level) and the transformer loading exceeds its threshold (102% vs 95%). A snapshot analysis increasing electricity consumption at the fuelling station by 1MW will lower the transformer loading by 17% using (5). The necessary increase in power input for the next minute at 08:51 to return loading to the threshold level is given by

$$\Delta P_{h2,t=8:51}^{+} = \frac{102\% - 95\%}{17\% \mathbin{/} \mathrm{MW}} = 0.41\mathrm{MW}$$

Due to this control, it can been seen that at 08:51 the increased electrolysis setpoint of $1.44\mathrm{MW}$ $(1.03\mathrm{MW} + 0.41\mathrm{MW})$ successfully reduces the transformer loading from 107% under no control to 100%. However, it still above the target threshold, due the rising wind speed in this minute partially counteracting the control effect. Thus, overproduction continues to be activated for 08:52, with an increased setpoint calculated as 1.74MW.

The actual loading at 08:52 turns out to be 93%, partly contributed by the reduced wind speed in this minute. This leaves 2% headroom for the fuel station to (partly) return from overproduction. Given that the accumulated overproduced hydrogen in the tanks from the previous time periods up to 8:52 has not been fully released ($E_{h2,t=8:50}^{acm} = 0.04$MWh), underproduction is activated from 08:53 to offset overproduction. The reduction aiming to release overcharged storage is calculated using (9) as

$$\Delta P_{h2,t}^{acm} = \frac{0.04MWh}{1min} = 2.4MW$$

but the final reduction is also subject to the available free headroom at the transformer which is estimated at 08:52 as

$$\Delta P_{h2,t}^{-} = \frac{95\% - 93\%}{20\%/\mathrm{MW}} = 0.1\mathrm{MW}$$

The required electrolysis input is therefore determined as 1.64 MW for 08:53 (1.74MW – 0.1MW). Figure 5 shows that at 08:53, while the electrolysis input is partly returned from overproduction, the transformer maintains a below target loading.

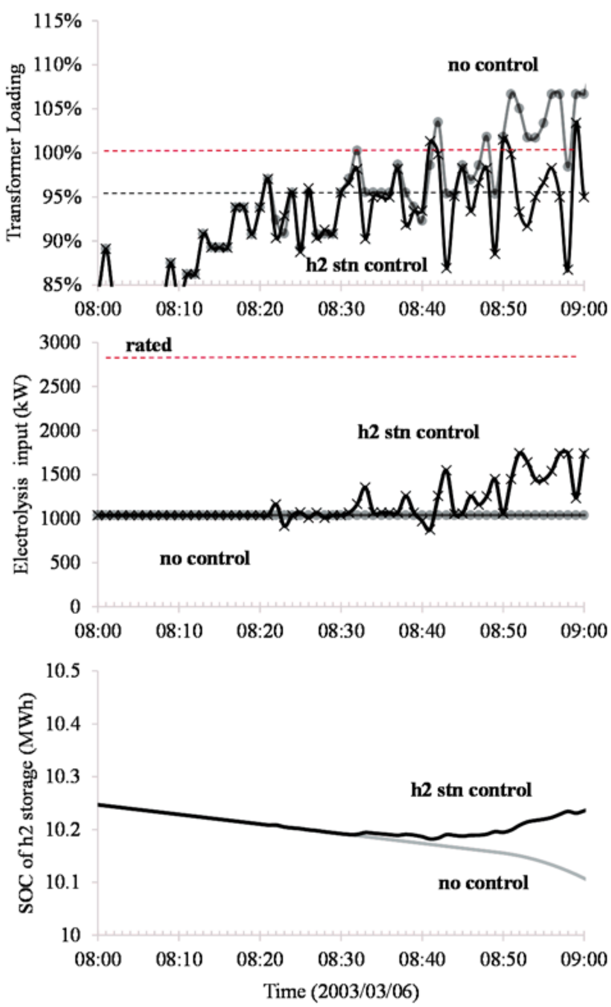

Figure 5. Transformer loading (top), electrolysis input at refuelling station (middle) and state of charge for hydrogen onsite storage (bottom) during 1 hour period simulation

Overall, Figure 5 shows that throughout the 1 hour window, when there is no overloading at transformer, the refueling station simply maintains its input. Once overloading occurs, a new operating point is calculated and the effective release of congestion can be seen. Thus, the duration of overloading is reduced to 3 minutes compared with 13 otherwise.

B. Validation of operation strategies for 5 days

To assess the performance of the operation strategy over a longer period of time, a 5-day sample window depicting network operation in winter with strong wind is studied. The primary transformer loading during the period under different scenarios of operation strategies is shown in Figure 6.

The initial scenario, referred as the 'no h2 stn', is considered without the refueling station, in order to benchmark any impact the connection of a refueling station may have. Clearly, a great amount of overloading events occur as expected due to the lack of the local consumption of DG output by the station. Comparing the base case with the passive operation results, termed as 'passive stn' in Figure 6 (top), shows that a considerable share of overloading during the day time is avoided due to the operation of the fuelling station electrolyser. The remaining thermal constraints during the night are partly mitigated once the fuelling station consumes electricity at a steady rate throughout the day ('steady stn' in Figure 6 bottom). Lastly, almost of all the overloading at the transformer is solved when the fuelling station is capable of real-time changes in scheduled electricity input by increasing hydrogen production during the period when the network is constrained in 'active stn scenarios' (Figure 6 bottom), and subsequently reducing its electricity input once the network is not constrained.

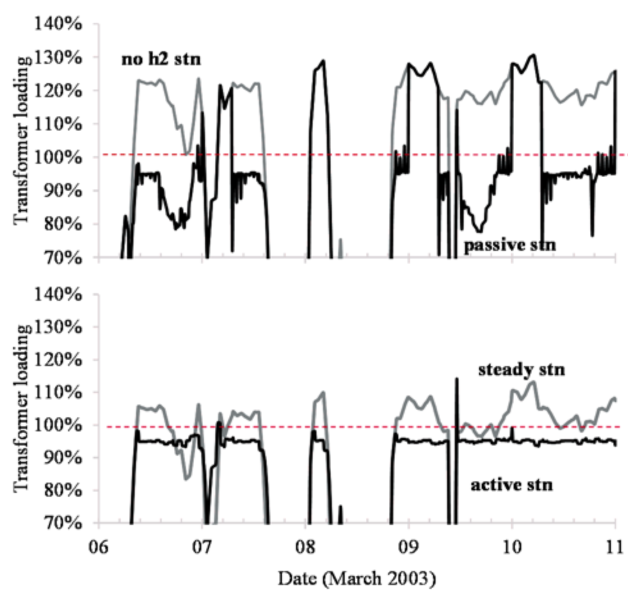

Figure 6. Transformer loading during 5 day period with strong wind under different operational strategies scenarios (base case and passive case at top; steady output and active operation case in bottom)

Using the active operation strategy effectively maintains the transformer loading below its limits even during strong wind periods. This means there is no or less need for other control schemes to manage this constraint, such as curtailment of wind output at bus C. The curtailment requirement in other operation scenarios is compared with the active strategy in Figure 7. It shows there is a maximum 92% reduction of curtailment by operating actively. If the transformer is allowed to tolerate short time overloading, the active operation fuelling station scheme can fully replace the needs for curtailment at bus C.

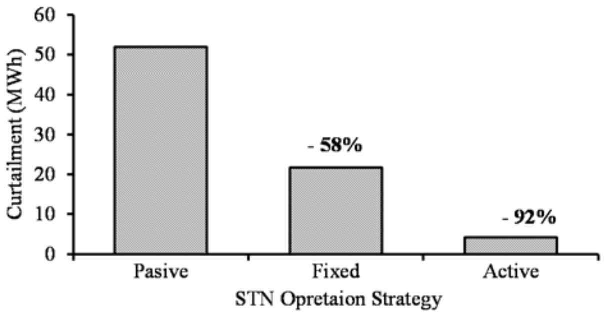

Figure 7. Curtailment requirement of wind farm at bus C under different hydrogen refuelling station cases

IV. Conclusion

The case study demonstrates that the active operation strategies of hydrogen refuelling stations are able to manage the overloading issue at the primary transformer caused by DG export. Over the study period, the active control of the refuelling station considerably reduces wind curtailment. Therefore, the effectiveness of the proposed active operation strategy of hydrogen fuelling stations to support renewable integration is validated. The implementation of this active scheme needs real-time measurements at the critical point of the network, and also adequate hydrogen storage tanks onsite. The work would be useful for better understanding the impact of deploying hydrogen fuelling stations and also motivating relevant stakeholders to explore its full value, especially by means of providing demand side management, ancillary services and deferring network reinforcement. In this way, hydrogen refuelling stations could potentially benefit the DNO and renewable developers, rather than just impose challenges. The planned work will study more complicated distribution networks where multiple refuelling stations exist and may require a certain amount of coordinated control.

V. Acknowledgements

The authors would like to thank Dr Paul E Dodds (UCL), Dr Phil Coker (University of Reading) and Dr Warren Hicks for helpful discussions and suggestions for this work.

References

[1] E4tech and Element Energy, *Hydrogen and Fuel Cells: Opportunities for Growth, A Roadmap for the UK* 2016.

[2] H. Xu, I. Kockar, S. Schnittger, and J. Rose, "Influences of Hydrogen Electrolyser Demand on Distrbuition Network Under Different Operational Constraints And Electricity Pricing Scenarios," *CIRED Workshop -Helsinki*, 2016.

[3] R. M. Oviedo, Z. Fan, and M. Sooriyabandara, "Ecoisland: A hydrogen refueler and storage system with renewable energy sources." pp. 1-5.

[4] A. A. Akhil, G. Huff, A. B. Currier, B. C. Kaun, D. M. Rastler, S. B. Chen, A. L. Cotter, D. T. Bradshaw, and W. D. Gauntlett, *DOE/EPRI Electricity Storage Handbook in Collaboration with NRECA*, United States, 2015.

[5] E. Rothuizen, and M. Rokni, "Optimization of the overall energy consumption in cascade fueling stations for hydrogen vehicles," *International Journal of Hydrogen Energy*, vol. 39, no. 1, pp. 582-592, Jan 2, 2014.

[6] E. Rothuizen, W. Merida, M. Rokni, and M. Wistoft-Ibsen, "Optimization of hydrogen vehicle refueling via dynamic simulation," *International Journal of Hydrogen Energy*, vol. 38, no. 11, pp. 4221-4231, Apr 15, 2013.

[7] H. Dagdougui, A. Ouammi, and R. Sacile, "Modelling and control of hydrogen and energy flows in a network of green hydrogen refuelling stations powered by mixed renewable energy systems," *International Journal of Hydrogen Energy*, vol. 37, no. 6, pp. 5360-5371, Mar, 2012.

[8] M. Kiaee, A. Cruden, D. Infield, and P. Chladek, "Utilisation of alkaline electrolysers to improve power system frequency stability with a high penetration of wind power," *IET Renewable Power Generation*, vol. 8, no. 5, pp. 529-536, Jul, 2014.

[9] S. Carr, G. C. Premier, A. J. Guwy, R. M. Dinsdale, and J. Maddy, "Hydrogen storage and demand to increase wind power onto electricity distribution networks," *International Journal of Hydrogen Energy*, vol. 39, no. 19, pp. 10195-10207, Jun 24, 2014.

[10] S. Carr, F. Zhang, F. Liu, Z. L. Du, and J. Maddy, "Optimal operation of a hydrogen refuelling station combined with wind power in the electricity market," *International Journal of Hydrogen Energy*, vol. 41, no. 46, pp. 21057-21066, Dec 14, 2016.

[11] Q. Zhou, and J. W. Bialek, "Generation curtailment to manage voltage constraints in distribution networks," *IET Generation, Transmission & Distribution*, vol. 1, no. 3, pp. 492-498, 2007.

[12] T. Sansawatt, L. F. Ochoa, and G. P. Harrison, "Smart Decentralized Control of DG for Voltage and Thermal Constraint Management," *IEEE Transactions on Power Systems*, vol. 27, no. 3, pp. 1637-1645, Aug, 2012.

[13] J. Robertson, G. Harrison, and A. R. Wallace, "OPF Techniques for Real-Time Active Management of Distribution Networks," *IEEE Transactions on Power Systems*, in press.

[14] J. Quiro-Tortos, L. F. Ochoa, S. W. Alnaser, and T. Butler, "Control of EV Charging Points for Thermal and Voltage Management of LV Networks," *IEEE Transactions on Power Systems*, vol. 31, no. 4, pp. 3028-3039, 2016.

[15] Argonne National Laboratory: Centre for Transportation Research, "H2A Delivery Scenario Analysis Model Version 3.0 (HDSAM 3.0) User's Manual. ," 2015.